# Whole-exome sequencing identifies multiple loss-of-function mutations of NF-κB pathway regulators in nasopharyngeal carcinoma

Hong Zheng[a,1], Wei Dai[a,1], Arthur Kwok Leung Cheung[a,1], Josephine Mun Yee Ko[a], Rebecca Kan[a], Bonnie Wing Yan Wong[a], Merrin Man Long Leong[a], Mingdan Deng[a], Tommy Chin Tung Kwok[a], Jimmy Yu-Wai Chan[b,c], Dora Lai-Wan Kwong[a,b], Anne Wing-Mui Lee[a,b], Wai Tong Ng[b,d], Roger Kai Cheong Ngan[b,e], Chun Chung Yau[b,f], Stewart Tung[b,g], Victor Ho-fun Lee[a,b], Ka-On Lam[a,b], Chung Kong Kwan[b,e], Wing Sum Li[b,e], Stephen Yau[e], Kwok-Wah Chan[h], and Maria Li Lung[a,b,2]

[a]Department of Clinical Oncology, The University of Hong Kong, Hong Kong, People's Republic of China; [b]Center for Nasopharyngeal Carcinoma Research, The University of Hong Kong, Hong Kong, People's Republic of China; [c]Department of Surgery, The University of Hong Kong, Hong Kong, People's Republic of China; [d]Department of Clinical Oncology, Pamela Youde Nethersole Eastern Hospital, Hong Kong, People's Republic of China; [e]Department of Clinical Oncology, Queen Elizabeth Hospital, Hong Kong, People's Republic of China; [f]Department of Oncology, Princess Margaret Hospital, Hong Kong, People's Republic of China; [g]Department of Clinical Oncology, Tuen Mun Hospital, Hong Kong, People's Republic of China; and [h]Department of Pathology, The University of Hong Kong, Hong Kong, People's Republic of China

Edited by Tak W. Mak, The Campbell Family Institute for Breast Cancer Research at Princess Margaret Cancer Centre, University Health Network, Toronto, ON, Canada, and approved August 5, 2016 (received for review May 12, 2016)

**Nasopharyngeal carcinoma (NPC) is an epithelial malignancy with a unique geographical distribution. The genomic abnormalities leading to NPC pathogenesis remain unclear. In total, 135 NPC tumors were examined to characterize the mutational landscape using whole-exome sequencing and targeted resequencing. An APOBEC cytidine deaminase mutagenesis signature was revealed in the somatic mutations. Noticeably, multiple loss-of-function mutations were identified in several NF-κB signaling negative regulators *NFKBIA*, *CYLD*, and *TNFAIP3*. Functional studies confirmed that inhibition of NFKBIA had a significant impact on NF-κB activity and NPC cell growth. The identified loss-of-function mutations in *NFKBIA* leading to protein truncation contributed to the altered NF-κB activity, which is critical for NPC tumorigenesis. In addition, somatic mutations were found in several cancer-relevant pathways, including cell cycle-phase transition, cell death, EBV infection, and viral carcinogenesis. These data provide an enhanced road map for understanding the molecular basis underlying NPC.**

nasopharyngeal carcinoma | somatic mutation landscape | NF-κB signaling | whole-exome sequencing | APOBEC-mediated signature

Nasopharyngeal carcinoma (NPC) is a malignancy characterized by geographic and etiologic features distinct from other head and neck cancers. Although worldwide, NPC is rare, it is highly prevalent in Southeast Asia and north Africa. The predominant WHO subtype of NPC in Asia is nonkeratinizing undifferentiated NPC. One critical etiological factor for NPC is EBV infection, marking it as one of the most important human virus-associated cancers (1). It is well-accepted that host genetics, EBV infection, and environmental factors together contribute to the pathogenesis of NPC.

NPC is a unique cancer that arises after the accumulation of a number of critical genetic and epigenetic events that contribute to tumor development (1). Previous studies suggest that the loss of chromosomes 3p and 9p regions is an early event for the transformation of the normal nasopharyngeal epithelium (2). The copy number losses in chromosomes 11q, 13q, 14q, and 16q and copy number gains in 11q and 12p are also frequently reported (1). Moreover, methylome studies of clinical samples reveal widespread methylation changes in NPC tumors (3). To characterize the genetic events in NPC, Lin et al. (4) performed whole-exome sequencing (WES) in NPC tumors and identified the somatic changes in chromatin modification, ErbB-PI3K signaling, and autophagy pathways. Interestingly, their study shows that *TP53* is the most frequently altered gene in NPC; however, mutations in this gene only account for 10.4% of the NPC cases. More than 40% of the cases have no alterations in the reported important cellular processes and pathways. Therefore, the overall picture of genetic changes underlying NPC tumorigenesis is still not fully elucidated. Thus, in this study, we sought to further characterize the somatic mutations in the Hong Kong NPC cases. We also used publicly available WES data to identify yet more critical genetic events in NPC pathogenesis. Improved understanding of the molecular changes in NPC provides a basis for the rational development of targeted therapies.

## Results

**WES of NPC.** We performed WES with 51 primary tumors and 8 recurrent tumors, 3 of which had matching lymph node metastatic tumors, and used targeted resequencing for an additional 73

### Significance

Host genetics, environmental factors, and EBV infection together contribute to nasopharyngeal carcinoma (NPC) development. A number of critical genetic and epigenetic events contributing to tumor development has been reported. However, the genomic alterations in NPC have not been completely deciphered. We used the whole-exome sequencing approach to study the somatic mutations in NPC, and an APOBEC-mediated mutagenesis signature was revealed. Importantly, multiple loss-of-function mutations in the NF-κB–negative regulators (*NFKBIA*, *CYLD*, and *TNFAIP3*) were discovered in NPC tumors, and we functionally confirmed that the *NFKBIA* loss-of-function mutations induce damaging effects on the WT proteins. Detection of these mutations emphasizes the critical role of NF-κB signaling in NPC tumorigenesis and provides perspectives for targeting this pathway in NPC treatment.

Author contributions: M.L.L. designed research; H.Z., W.D., A.K.L.C., J.M.Y.K., R.K., B.W.Y.W., M.M.L.L., M.D., T.C.T.K., J.Y.-W.C., D.L.-W.K., A.W.-M.L., W.T.N., R.K.C.N., C.C.Y., S.T., V.H.-f.L., K.-O.L., C.K.K., W.S.L., S.Y., and K.-W.C. performed research; B.W.Y.W. provided samples and clinical information; J.Y.-W.C., D.L.-W.K., A.W.-M.L., W.T.N., R.K.C.N., C.C.Y., S.T., V.H.-f.L., K.-O.L., C.K.K., W.S.L., and S.Y. provided samples; H.Z., W.D., A.K.L.C., and K.-W.C. analyzed data; and H.Z., W.D., A.K.L.C., and M.L.L. wrote the paper.

The authors declare no conflict of interest.

This article is a PNAS Direct Submission.

Data deposition: The sequences reported in this paper has been deposited in the National Center for Biotechnology Information Sequence Read Archive, www.ncbi.nlm.nih.gov/sra (accession nos. SRA288429 and SRA291304).

[1]H.Z., W.D., and A.K.L.C. contributed equally to this work.

[2]To whom correspondence should be addressed. Email: mlilung@hku.hk.

This article contains supporting information online at www.pnas.org/lookup/suppl/doi:10.1073/pnas.1607606113/-/DCSupplemental.



GENETICS

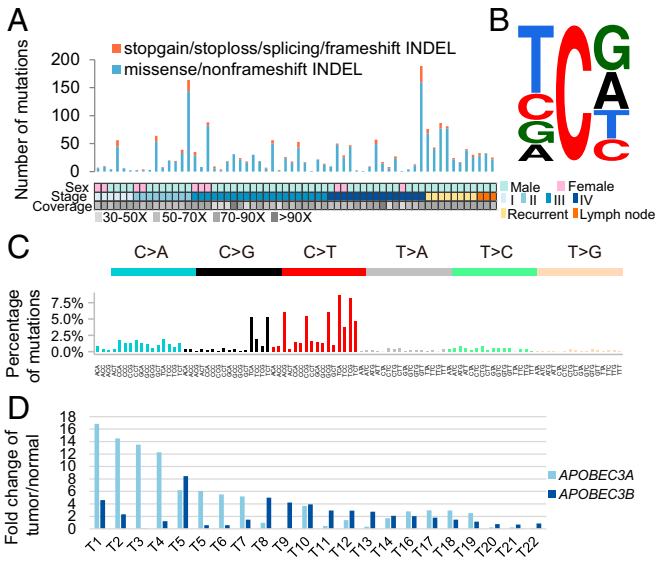


**Fig. 1.** Somatic mutation rates and signatures in NPC. (*A*) Number of nonsilent somatic mutations in NPC tumors. (*B*) Trinucleotide contexts of somatic mutations occurring at cytosine nucleotides in NPC. The font sizes of the nucleotides at the 3′ and 5′ positions are proportional to their frequencies. (*C*) Mutational signatures are displayed according to 96 substitution classification defined by the substitution class and sequence context immediately before and after the mutated base (9). Vertical axis displays percentage of mutations attributed to a specific mutation type. The trinucleotide contexts of the mutated bases are shown on the *x* axis. (*D*) Expressions of *APOBEC3A* and *APOBE3B* evaluated by qRT-PCR in an additional 22 tumor pairs.

primary tumors (*SI Appendix*, Table S1). Paired blood samples were also sequenced as references. RNA sequencing (RNASeq) was performed in 10 tumor pairs with adequate quality and quantity of RNA. The overall workflow is shown in *SI Appendix*, Fig. S1*A*. After removing duplicates, the mean target coverages of tumor and blood samples were 70× and 49× in WES (12% average duplication rate) and 190× and 68× in targeted resequencing (9% average duplication rate), respectively. For tumor samples in WES, 72% of bases were covered at least 30×, and 50% of bases were covered at least 50× (*SI Appendix*, Fig. S1*B* and Table S2). Overall, 1,374 nonsilent somatic mutations that change the protein sequences or involve splice sites in 1,242 genes were identified across 51 primary tumors, and 457 nonsilent somatic mutations in 438 genes were identified in recurrent and metastatic tumors by WES (Fig. 1*A* and *SI Appendix*, Tables S3 and S4). Subsequently, in total, 186 nonsilent somatic mutations in 123 genes were identified across 73 primary tumors in targeted resequencing (*SI Appendix*, Table S5). In our study, the median mutation rate of NPC is 0.9 somatic mutations per megabase in coding regions (*SI Appendix*, Fig. S2). Somatic mutations were verified by Sanger sequencing or RNASeq, and a verification rate of 95% was achieved (*SI Appendix*, Table S6).

To identify potential driver events in tumorigenesis, we combined data from WES and targeted resequencing. MutSigCV (5) analysis revealed two significantly mutated genes, NFKB inhibitor alpha (*NFKBIA*) and tumor protein p53 (*TP53*) ($q < 10^{-10}$) (*SI Appendix*, Table S7). The top 100 genes from MutSigCV ranking were used for pathway and gene ontology analysis, which identified several pathways/terms with enriched somatic mutations, including cell cycle-phase transition, cell death, EBV infection, viral carcinogenesis, and the canonical NF-κB pathway (Fig. 2 and *SI Appendix*, Table S8). Several mutated genes are in the regions with frequent genomic losses previously reported in NPC (6–8), including 3p, 9q, 11q, 14q, and 16q (*SI Appendix*, Table S9).

**APOBEC-Mediated Signature Observed in NPC Tumors.** To identify the mutational signatures in NPC, the nonnegative matrix factorization approach was applied (9). Two mutational signatures were observed in NPC, including the ubiquitous signature in cancer characterized by C > T transitions predominantly occurring at NpCpG trinucleotides, which is generally attributed to spontaneous deamination of 5-methyl-cytosine, and the apolipoprotein B mRNA-editing enzyme, catalytic polypeptide-like (APOBEC)-mediated signature characterized by C > G and C > T mutations at TpCpN trinucleotides, which has never been reported in NPC before (Fig. 1 *B* and *C* and *SI Appendix*, Fig. S3). The APOBEC family of cytidine deaminases, particularly *APOBEC3B* and *APOBEC3A*, has been suggested as a source of mutations in multiple human cancers (10, 11). Consistently, RNASeq analysis showed up-regulation of *APOBEC3A*, *APOBEC3B*, or *APOBEC3A_B* (*APOBEC3A* and *APOBEC3B* deletion hybrid containing the promoter and coding region of *APOBEC3A* and the 3′ UTR of *APOBEC3B*) in tumor samples with APOBEC-mediated signatures observed (Fisher's exact test for enrichment, $P = 0.028$) (*SI Appendix*, Fig. S4). Quantitative PCR of additional NPC tumors showed that *APOBEC3A* or *APOBEC3B* was up-regulated in 86% (Fig. 1*D*). The APOBEC-mediated signature may provide additional clues for understanding the pathogenesis of NPC.

**Multiple Truncating Mutations in NF-κB Pathway-Negative Regulators.** Strikingly, multiple loss-of-function [LOF; including stopgain, frameshift insertions and deletions (INDELs), and splicing] mutations were detected in the NF-κB pathway-negative regulators, including *NFKBIA*, CYLD lysine 63 deubiquitinase (*CYLD*), and TNF alpha-induced protein 3 (*TNFAIP3*). In total, mutations in these negative regulators occurred in 7.3% of NPC primary tumors (Fig. 3*A* and *SI Appendix*, Fig. S5).

*NFKBIA* is the top candidate from MutSigCV analysis, and LOF mutations (E40fs-ins, E128X, Q165X, L236fs-ins, L236fs-del, and R245fs-del) in this gene were detected in six primary tumors. None of these mutations in this gene have been identified before. Two additional frameshift INDELs (L148fs-ins and L163fs-del) were also seen in primary tumors in previous WES studies of NPC (4, 12). Another negative regulator of the NF-κB pathway having multiple LOF mutations is CYLD, which cleaves the lysine 63-linked polyubiquitin chains from target proteins, including NEMO [IκB kinase (IKK) complex], TNF receptor-associated factor 2 (TRAF2), and TRAF6. By deubiquitination

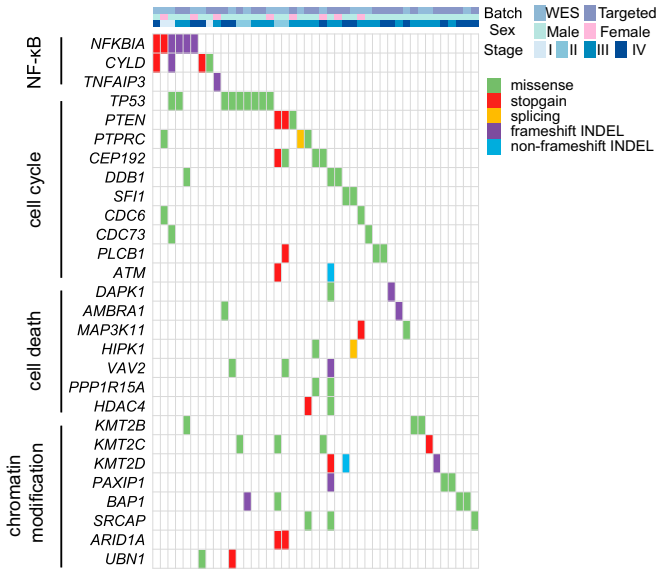


**Fig. 2.** Landscape of somatic mutations in NPC. The matrix shows important mutated genes and their associated pathways in NPC primary tumors analyzed by WES and targeted resequencing. Genes are shown on left-hand side. Only genes with detectable expression in RNASeq analysis are shown. Each column represents one tumor.

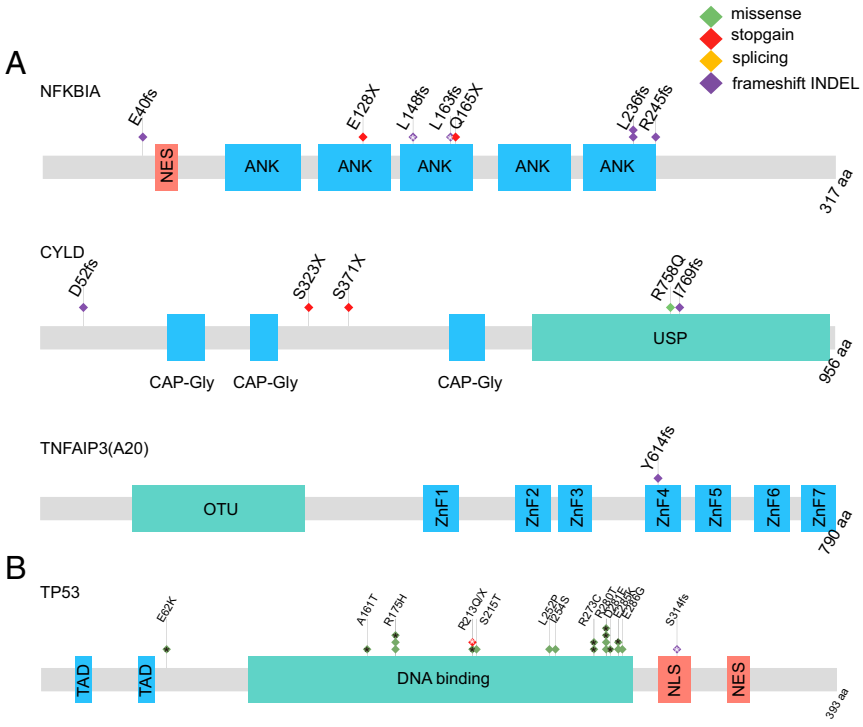


**Fig. 3.** Significantly mutated genes and relevant pathway in NPC. (*A*) Schematics of NF-κB pathway genes *NFKBIA*, *CYLD*, and *TNFAIP3* showing the positions of individual somatic mutations identified in NPC. (*B*) Schematics of *TP53* mutations. Each diamond represents one tumor. Protein domain and region information is obtained from the UniProt database. ANK, ankyrin repeat; CAP-Gly, cytoskeleton-associated proteins–Gly-rich domain; fs, frameshift mutation; NES, nuclear export signal; NLS, nuclear localization signal; OTU, ovarian tumor domain; TAD, transactivating domain; USP, ubiquitin-specific protease domain; X, stopgain mutation; ZnF1-7, Zinc finger domain 1–7. *Somatic mutations from previous WES studies (4, 12).

of IKK and its upstream regulators, CYLD negatively regulates NF-κB activation (13) (*SI Appendix*, Fig. S5*C*). Loss of *CYLD* expression can be observed in different types of human cancers, and it is now well-established that *CYLD* acts as a tumor suppressor gene (14). Expression of *CYLD* was also down-regulated in NPC (*SI Appendix*, Fig. S6 *A* and *B*). Four somatic mutations of *CYLD* (D52fs-del, S323X, S371X, and R758Q), including three LOF mutations, were detected in NPC primary tumors. Interestingly, a frameshift INDEL (I769fs-ins) was also detected in the mouse xenograft X666 as well as the C666 cell line (*SI Appendix*, Fig. S6 *C* and *D*). None of the LOF mutations in *CYLD* were previously identified, except the S371X, which was reported in a previous head and neck cancer case (15). Moreover, a frameshift mutation (Y614fs-del) in the NF-κB inhibitor, *TNFAIP3*, was detected in one NPC specimen, possibly leading to malfunction of its inhibition activity. This gene is known to modulate inflammatory signaling cascades and act as a critical tumor suppressor in various lymphomas (16).

***NFKBIA* LOF Mutations Influence the WT *NFKBIA* Function.** Because *NFKBIA* was the top candidate from MutSigCV analysis and the frequency of LOF mutations in this gene was the highest in NPC, it was selected for additional functional investigation. *NFKBIA* encodes IκBα, which belongs to the NF-κB inhibitor family (IκBs). Normally, NF-κB transcription factors are retained in the cytoplasm through binding to IκBs. In response to various signals, IκBs are phosphorylated by the IKK complex and degraded, which allows NF-κB to translocate into the nucleus and activate target genes (17) (*SI Appendix*, Fig. S5*C*). Our previous study (18) suggested the tumor-suppressive role of IκBα in NPC cells. Overexpression of the IκBα superrepressor induces significant in vitro and in vivo tumor-suppressive effects. We further investigated the effects of inhibition of IκBα in NPC cells by shRNA knockdown of *NFKBIA* in both HONE1 and HK1 NPC cell lines (Fig. 4*A*). Consistent with previous findings, there were significant increases of in vitro cell proliferation (Fig. 4*B*) and colony-forming abilities (Fig. 4*C*) after *NFKBIA* knockdown. This result further confirms the critical effect of IκBα inactivation or inhibition in NPC tumorigenesis. Based on in silico analysis (Fig. 4*D*) and site-directed mutagenesis followed by Western blotting analysis (Fig. 4*E*), all six LOF mutations in *NFKBIA* identified in our cohort were confirmed to induce premature stop codons. Five of six mutations resulted in the formation of truncated IκBα proteins with loss in the ankyrin (ANK) domains that are important for the interaction between the IκBα and NF-κB proteins (19). The effect of the IκBα inhibition on NF-κB activities was confirmed by using an NF-κB–specific dual luciferase promoter assay. Inhibition of the IκBα significantly increased NF-κB–specific promoter activities (Fig. 4*F*). The damaging effects of the mutations to the IκBα function were investigated by examining the NF-κB–specific promoter activities. Overexpression of the WT IκBα (IκBα-WT) and several IκBα mutants (E40fs-ins, E128X, Q165X, L236fs-ins, L236fs-del, and L245fs-del) in the 293T cells showed that IκBα-WT significantly suppressed NF-κB activities, whereas the IκBα-E40fs-ins, IκBα-E128X, and IκBα-Q165X resulting in dramatic IκBα truncation failed to inhibit the NF-κB activities (Fig. 4*G*). For the IκBα-L236fs-ins and IκBα-L236fs-del mutants, there was an enhanced NF-κB activity compared with the WT constructs, but the NF-κB activities were still slightly lower than the vector-alone (VA) control. The IκBα-L245fs-del mutant, which has only one-amino acid loss in the ANK domain, showed similar NF-κB activities as the IκBα-WT (Fig. 4*G*). The results provide functional evidence to support the damaging effects of at least three observed mutations to the IκBα protein function.

**Other Important Genes/Pathways Dysregulated by Somatic Mutations in NPC.** In addition to *NFKBIA*, *TP53* is another significantly mutated gene in NPC. Previous evidence suggested that alterations of *TP53* were unlikely to be involved in NPC primary tumors (20). However, *TP53* is the most frequently mutated gene in our cohort, with 9 of 124 primary tumors (7.3%) harboring missense mutations. The frequent mutations of *TP53* were also seen in the previous WES study (10.4%, considering somatic SNPs and INDELs) (4). Almost all somatic mutations fall into the DNA binding domain of *TP53*, including well-known hotspot and gain-of-function mutations (Fig. 3*B* and *SI Appendix*, Fig. S7*A*). Three tumor samples with *TP53* missense mutations were subjected to immunohistochemical (IHC) staining, and all showed high p53 expression (*SI Appendix*, Fig. S7*B*).

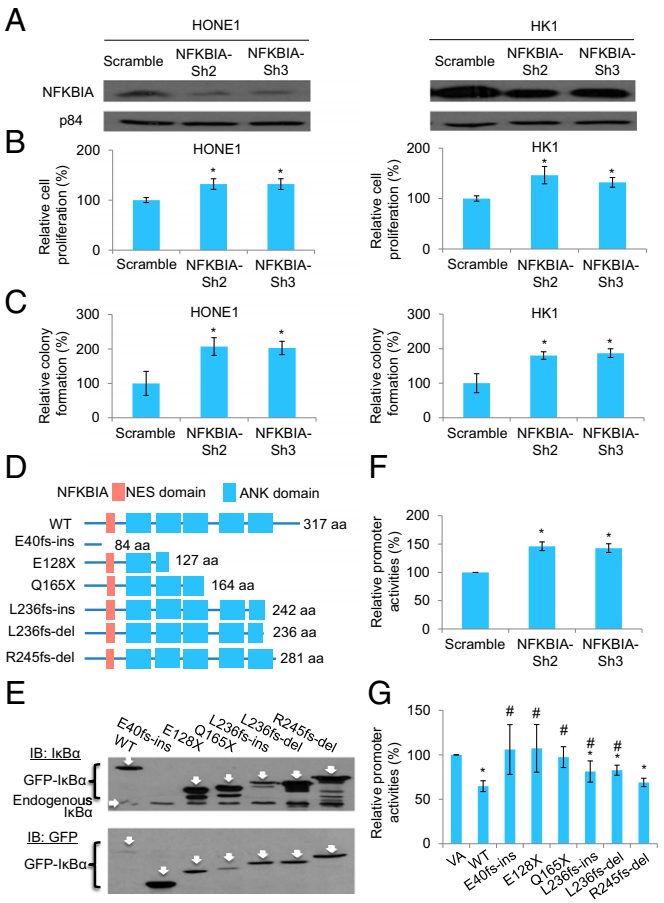


**Fig. 4.** Functional investigation of *NFKBIA* knockdown in NPC cells and the truncating mutations identified in the IκBα protein. (*A*) Expression of IκBα protein in both NPC HONE1 and HK1 cell lines after knockdown with two independent sets of shRNA knockdown oligonucleotides. (*B*) Cell proliferation assay of HONE1 and HK1 cells after *NFKBIA* knockdown. The relative cell proliferation rate was compared with the corresponding scramble control. (*C*) Colony formation assay of HONE1 and HK1 cells after *NFKBIA* knockdown. (*D*) Schematic diagram illustrates the truncated site of each mutant of IκBα protein by in silico analysis. NES, nuclear export signal. (*E*) Western blot results illustrate the protein size of each mutant. The IκBα was tagged with an N-terminal GFP tag. The GFP-IκBα-WT (61.9 kDa), GFP-E40fs-ins (35.659 kDa; this mutant lost the epitope for the IκBα antibody recognition; therefore, it cannot be detected by the IκBα-specific antibody), GFP-E128X (41.68 kDa), GFP-Q165X (45.49 kDa), GFP-L236fs-ins (53.84 kDa), GFP-L236fs-del (53.04 kDa), and GFP-R245fs-del (57.85 kDa) were detected by specific antibody against the (*Upper*) IκBα and (*Lower*) GFP. IB, immunoblot. (*F*) NF-κB–specific dual luciferase promoter assay in the 293T cell lines with *NFKBIA* knockdown. (*G*) NF-κB–specific dual luciferase promoter assay in the 293T cell line with expression of IκBα-WT and mutants. This cell line has constitutive NF-κB activation. The relative promoter activity value was compared with the VA control. The data shown in *B*, *C*, *F*, and *G* represent means ± SD ($n = 3$). *Statistical significance ($P < 0.05$) compared with the scramble control or VA; #statistical significance ($P < 0.05$) compared with the WT.

Epigenetic regulators are frequently mutated in cancers, and somatic alterations of the chromatin modification pathway have been implicated in NPC previously (4). Apart from previously reported *ARID1A*, *BAP1*, *KMT2C*, *KMT2D*, *KMT2B*, *EP300*, *EP400*, *HUWE1*, *SRCAP*, and *UBN1*, we also discovered mutations in new players, including *HDAC4*, *PAXIP1*, *CABIN1*, *DDB1*, and *KAT6B* (Fig. 2 and *SI Appendix*, Fig. S8). To fully exploit the available sequencing data, we combined the somatic mutations in WES samples from this study and the previous study (4) (combined sample size = 116), and performed MutSigCV analysis (*SI Appendix*, Table S10). *NFKBIA* and *TP53* remained the top candidates followed by *BAP1*, with $q$ values less than 0.2. Among the top 142 genes with $P$ values less than 0.05, 35 genes were identified in both studies. Noticeably, four of these (*TP53*, *NFKBIA*, *CD44*, and *CR2*) are related to the EBV infection pathway. *CR2* is also known as *CD21*, which encodes a membrane receptor for EBV on B lymphocytes (21). Mutations in *CD44* were also found in both the recurrent and lymph node metastatic tumors from one NPC case.

## Discussion

NPC is an intriguing model for investigating the complex interaction between host genetics, environmental factors, and viruses during tumorigenesis. The somatic mutations detected in tumors reflect multiple mutagenic processes operative through cancer development. Depending on the different carcinogenic agents and DNA repair mechanisms, these mutagenic processes imprint distinct patterns on the cancer genome and are characterized by a set of mutational signatures. Up to 21 mutational signatures have been deciphered across human cancers, revealing multiple mutagenic mechanisms, including exogenous agents, such as tobacco carcinogens and UV light, as well as endogenous deficiency in DNA repair mechanisms (9). In NPC, we now report the identification of the APOBEC-mediated signature. This signature had not been reported in the earlier WES study (4). However, we identified one specimen in their study, which was an outlier with a high number of C > T mutations at GpCpG trinucleotides, that obscured direct observation of the signature composition. Moreover, using the nonnegative matrix factorization approach (9), we identified the APOBEC-mediated signature from that dataset (*SI Appendix*, Fig. S9). We reported an up-regulation of *APOBEC3A* and *APOBEC3B* in the tumor samples with APOBEC-mediated signatures. A trend of up-regulation of *APOBEC3B* in NPC tumors was also shown in the previous WES study using a public microarray dataset (22), although the difference did not reach the statistical significance ($P = 0.086$, Mann–Whitney $u$ test). The APOBEC mutational process has been shown to foster subclonal expansions and propagate intratumor heterogeneity in several cancers (23). The subclonal driver mutations contribute to tumor maintenance, adaption, and immune escape (11). There have been ongoing efforts to develop small molecule inhibitors to target APOBEC3 family members (24). The APOBEC enzymes serve as potential drug targets to suppress APOBEC-mediated mutagenesis and attenuate tumor evolution and adaptation. Thus, it is of interest that this characteristic signature is found in NPC.

Multiple pathways that are potentially relevant to NPC are dysregulated by somatic mutations, including cell cycle-phase transition, cell death, EBV infection, viral carcinogenesis, and the NF-κB pathway. It is of interest that *TP53* is the most frequently mutated gene in NPC, although earlier studies had reported only infrequent *TP53* mutations in this cancer (20). Using the powerful WES approaches, we now detect mutations in 7.3% of NPC biopsies. However, this frequency is still low compared with other human cancers, in which a much higher frequency of *TP53* mutations is observed (25). Interestingly, the overall frequency of somatic mutations in NPC is rather low, which may be intrinsic to NPC and may, in part, be because of the fact that, in addition to the somatic changes, widespread epigenetic alterations are observed in NPC, another important mechanism contributing to NPC tumorigenesis. In our earlier studies, we detected a higher frequency of promoter hypermethylation in NPC compared with many other human cancers. The frequent methylation may be contributed, in part, by the ability of EBV to play an important role in reprogramming host gene expression. The essential contributing role of EBV in the tumorigenesis process is compelling and warrants additional investigation to unravel the molecular genetic basis of NPC in which host genetics and EBV infection play an important causal role. Integration of "omics" data from WES, methylome, and transcriptome analyses is expected to further contribute to elucidating this interplay between host and virus. It is also possible that the commonly observed infiltration of intratumoral lymphocytes in NPC may limit the ability to detect some somatic mutations that are present in only a small fraction of the population of the cancer cells.

NF-κB signaling has been extensively implicated in NPC, with constitutive activation detected in NPC cell lines and primary tumors (26). Several mechanisms have been proposed for NF-κB signaling activation in NPC. The EBV oncoprotein LMP1 activates both the canonical and noncanonical NF-κB pathways in NPC (27). In addition, somatic alterations in NF-κB pathway regulators have been reported in NPC, including frameshift and missense mutations of *TRAF3*, *TRAF2*, and *TNFAIP3* in 3 of 33 (9.1%) primary tumors, large deletions of *NFKBIA* and *TRAF3*, and frameshift mutation of *TRAF3* in NPC xenografts and cell line (26). These genetic alterations potentially contribute to the altered NF-κB activity in NPC. In this study, multiple LOF mutations in NF-κB–negative regulators were identified. The *NFKBIA* LOF mutations induce truncation of IκBα and cause the loss of ANK domains, which are important for IκBα binding with NF-κB. Disruption of this binding by truncating mutations promotes nuclear translocation of NF-κB, thus activating the transcription of downstream targets. The impact of the mutations on the regulation of the NF-κB activities was validated, and IκBα mutants showed decreased ability to inhibit the NF-κB activity. In addition, another crucial NF-κB–negative regulator, CYLD, has a C-terminal deubiquitinase domain. The loss of this important domain caused by the LOF mutations results in the defective deubiquitination ability of CYLD and greatly affects its tumor-suppressive function.

*NFKBIA* mutations are observed in various cancers, whereas LOF mutations of *NFKBIA* are rare in the solid tumors (*SI Appendix*, Fig. S10*A*). Across The Cancer Genome Atlas data comprised of over 11,000 solid tumors, only three LOF mutations were detected in this gene (E302X, breast cancer; R140X, melanoma; and X112_splice, glioma) (28). Our study shows that the prevalence of *NFKBIA* mutations, especially LOF mutations, is high in NPC. In addition to NPC, previous studies indicate that EBV is associated with a subset of Hodgkin's lymphoma, diffuse large B-cell lymphoma (DLBCL), and gastric cancers (29, 30). Constitutive NF-κB activation is a hallmark of Hodgkin's lymphoma and also observed in a subset of clinical samples in DLBCL and gastric cancer (31, 32). Interestingly, the increased prevalence of *NFKBIA* mutations is also observed in DLBCL (6.3%; 3 of 48 cases) (28) and Hodgkin's lymphoma (37.5%; 6 of 16 cases) (33). Moreover, *NFKBIA* LOF mutations are reported in 2.1% of DLBCL cases and 18.8% of Hodgkin's lymphomas. Likewise, LOF mutations of *TNFAIP3* are also present at a high frequency in DLBCL cases (12.5%; 6 of 48 cases) (*SI Appendix*, Fig. S10*B*), and LOF mutations in *CYLD* are often reported in gastric and head and neck cancers (*SI Appendix*, Fig. S10*C*). The other NF-κB regulator, *TRAF3*, is reported to have LOF mutations in NPC (26). In addition, LOF mutations in *TRAF3* are also found in head and neck and gastric cancers (15, 34). It is interesting to speculate whether the genetic alterations in these NF-κB regulators may be one of the mechanisms underlying the dysregulation of NF-κB signaling in several virus-associated malignancies; however, more rigorous studies would be needed to determine the verity of this possibility. Importantly, our findings provide an opportunity for potential therapeutic exploitation in NPC. Previous studies indicate that the NF-κB pathway is a potential therapeutic target in cancer treatment (35). Given the frequency of aberrant activation of this pathway in NPC, NF-κB signaling inhibitors may be promising therapeutics for NPC. Our study provides an enhanced road map for understanding the molecular basis underlying NPC and has identified targetable signaling pathways for targeted therapies in NPC.

## Methods

**Sample Acquisition.** Tumor and blood samples were collected by the Area of Excellence Hong Kong NPC Tissue Bank from Queen Mary, Queen Elizabeth, Princess Margaret, Tuen Mun, and Pamela Youde Nethersole Eastern Hospitals. Informed consent for sample collection was obtained according to protocols approved by the Institutional Review Board of The University of Hong Kong. The quality of tumor samples was examined by tissue sectioning and H&E staining to estimate the tumor content (*SI Appendix*, Fig. S11 and Table S1). Only the best quality samples with 30–90% tumor content were chosen for subsequent study. DNA was extracted from the fresh-frozen biopsies and peripheral blood lymphocytes using the AllPrep DNA/RNA Micro Kit (Qiagen) and the QIAamp DNA Blood Mini Kit (Qiagen), respectively. The genomic DNA was analyzed on 0.7% agarose gels for quality control. The quantity and quality of the genomic DNA were assessed by Nanodrop 1000 (Thermo Scientific) and Qubit (Life Technologies), respectively.

**Power of Study Design.** In the discovery stage, we aimed to detect the mutated genes with a mutation rate of 5%. The power estimation was performed using the method described previously (36). The probability that no sample has any mutation in gene G is $(1 - x)^N$, where $N$ indicates the number of samples sequenced in the study, and $x$ indicates the fraction of all tumor samples having gene G mutated. The probability of observing gene G mutated at least once was $1 - (1 - x)^N$, which is 93% for 51 discovery samples, assuming $x = 5\%$. Likewise, the probability of observing gene G mutated twice or more was $1 - (1 - x)^N - N(1 - x)^{(N - 1)}x$, which is 73% for 51 discovery samples, assuming $x = 5\%$.

**WES and Targeted-Resequencing Data Analysis.** The procedure of library preparation and sequencing for WES and targeted resequencing is found in *SI Appendix, SI Materials and Methods*. Sequencing reads were quality checked and aligned to the human genome (hg19) with BWA (37). Picards were applied to sort output bamfiles and mark duplicates. GATK (38) was applied for paired local realignment around INDELs, base quality recalibration, and variants discovery according to GATK Best Practices recommendations (39, 40). Quality of germline variants was checked by GATK and PLINK (41, 42) to remove unmatched tumor pairs and abnormal samples having either low-sequencing coverage or an extremely high number of germline variants or contamination. All of the samples in this study passed this process of quality check. Somatic SNPs and INDELs were called using MuTect (43) and VarScan2 (44), respectively. Somatic mutations were kept if there were no fewer than five reads supporting a mutant allele in tumor samples or the mutant allele frequency was more than 10%. Somatic mutations were further filtered if they are present in public databases (1000G and ESP6500) or in-house controls (>1,000) with minor allele frequency more than 1%. Recurrent somatic mutations and low-quality mutations (mutant allele frequency less than 10% or fewer than five reads supporting mutant allele in tumor samples) in recurrently mutated genes were manually checked in Integrative Genomics Viewer (IGV) alignment to further remove false positives based on mapping quality, base Phred quality score, and quality of adjacent regions. The WES data from the previous study (4) were also analyzed following the same pipeline.

We identified candidate genes for targeted resequencing that fulfilled the following criteria: (*i*) genes that harbor nonsilent somatic mutations in at least two NPC tumors or have LOF (i.e., stopgain, splicing, or frameshift INDELs) mutations (*ii*) excluding problematic genes or variant locations, which are likely to be false positive signals in WES (45), and (*iii*) excluding genes that are not expressed in NPC and normal nasopharynx tissues based on RNASeq data of 10 tumor/normal pairs (mean fragments per kilobase per million less than one and not expressed in 50% of the samples). This filtering process generated 211 potential candidate genes. Together with candidate genes in our genetic susceptibility study of NPC (46), in total, 346 genes were subjected to targeted resequencing in additional NPC cases.

**Mutation Verification.** Mutations were verified by either Sanger sequencing or RNASeq data from the same tumor pairs. For Sanger sequencing, PCR amplification was performed using FastStart Taq DNA polymerase with 50 ng genomic DNA as template. Primer sequences are listed in *SI Appendix*, Table S11.

**Mutational Signature Analysis.** Mutational signatures were deciphered using the nonnegative matrix factorization approach supplied in the Wellcome Trust Sanger Institute Mutational Signature Framework (9).

**Driver Events Identification.** Somatic mutations (including nonsilent, silent, and noncoding mutations) in 346 genes from tumors in both WES and targeted resequencing were input for MutSigCV (5) analysis and supplied with DNA replication time and chromatin state (open/closed) for each gene as well as level of transcription activity in NPC inferred from RNASeq data. Combined MutSigCV analysis of WES data from this study and the previous WES study followed similar procedures.

**IHC Staining.** IHC staining for p53 was performed using Anti-Human p53 Protein (Clone DO-7; Code No. M 7001; Dako) as previously described (18).

**Real-Time Quantitative RT-PCR.** The quantitative RT-PCR (qRT-PCR) was performed by using the FastStart Universal SYBR Green Master Mix (Roche) with gene-specific primers and GAPDH-specific primers as the control. Primer sequences are in *SI Appendix*, Table S11.

**Cell Culture and Expression Constructs.** The NPC EBV-negative HONE1 and HK1 and 293T cell lines were cultured with DMEM and supplemented with 5% (vol/vol) FBS, 5% (vol/vol) newborn calf serum, and 1% (vol/vol) penicillin/streptomycin (Life Technologies). The NFKBIA knockdown oligonucleotides were cloned into the pLKO.1-TRC cloning vector (gift from David Root, Broad Institute, Cambridge, MA; no. 10878; Addgene) (47), and the knockdown of NFKBIA gene was performed as described (18). For the expression of the WT and mutant constructs, the WT N-terminal GFP-tagged NFKBIA was cloned into the pCR3.1 expression vector (pCR3.1-GFP-NFKBIA; Life Technologies). The mutant constructs were established by using the site-directed mutagenesis method with the GeneArt Site-Directed Mutagenesis System (Life Technologies).

**In Vitro Cell Proliferation and Colony Formation Assays.** For the cell proliferation assay, in total, 3,000 cells were seeded into each well of a 96-well cell culture plate as previously described (48). The cell proliferation rate was measured by adding the 3-(4,5-dimethylthiazol-2-yl)-2,5-diphenyltetrazolium bromide solution to the cells and incubating for 3 h. The media were removed, and DMSO was used to dissolve the dye; results were measured by the microplate reader (Biotek). The colony formation assay was performed as described (18); in total, 8,000 cells were seeded into each well of a six-well cell culture plate. After incubation, the cells were fixed with formaldehyde and stained with the Giemsa.

**Western Blotting.** The Western blot experiments were performed as described (48). The antibodies against the IκBα and GFP proteins (Cell Signaling) were used to detect the expression of the targeted proteins, and the antibody against the p84 protein (GeneTex) was used as a loading control.

**NF-κB–Specific Dual Luciferase Promoter Assay.** The pT-FER reporter harbors the NF-κB binding elements. The binding of the NF-κB will result in activation of expression of the firefly luciferase. The EF1α promoter on the same vector drives the Renilla luciferase expression to serve as a normalization control. The NF-κB reporter gene consists of five repeats of the NF-κB consensus sequence (5′-TGGGGACTTTCCGC-3′) linked with a TATA box sequence. The promoter assay was performed in 293T cells, which has constitutive NF-κB activation, as we previously described (49).

**ACKNOWLEDGMENTS.** We thank the clinicians at the Queen Mary Hospital, Pamela Youde Nethersole Eastern Hospital, Queen Elizabeth Hospital, Princess Margaret Hospital, and Tuen Mun Hospital for collecting all of the samples used in this study. We also thank the Tissue Bank from the Area of Excellence Centre for NPC Research for providing the clinical samples for this study. This work was supported by Research Grants Council of the Hong Kong Special Administrative Region, People's Republic of China Grant AoE/M-06/08 (to M.L.L.).

1. Bruce JP, Yip K, Bratman SV, Ito E, Liu FF (2015) Nasopharyngeal cancer: Molecular landscape. *J Clin Oncol* 33(29):3346–3355.
2. Lo KW, Chung GT, To KF (2012) Deciphering the molecular genetic basis of NPC through molecular, cytogenetic, and epigenetic approaches. *Semin Cancer Biol* 22(2):79–86.
3. Dai W, et al. (2015) Comparative methylome analysis in solid tumors reveals aberrant methylation at chromosome 6p in nasopharyngeal carcinoma. *Cancer Med* 4(7):1079–1090.
4. Lin DC, et al. (2014) The genomic landscape of nasopharyngeal carcinoma. *Nat Genet* 46(8):866–871.
5. Lawrence MS, et al. (2013) Mutational heterogeneity in cancer and the search for new cancer-associated genes. *Nature* 499(7457):214–218.
6. Fang Y, et al. (2001) Analysis of genetic alterations in primary nasopharyngeal carcinoma by comparative genomic hybridization. *Genes Chromosomes Cancer* 30(3):254–260.
7. Chien G, Yuen PW, Kwong D, Kwong YL (2001) Comparative genomic hybridization analysis of nasopharygeal carcinoma: Consistent patterns of genetic aberrations and clinicopathological correlations. *Cancer Genet Cytogenet* 126(1):63–67.
8. Hui AB, et al. (1999) Detection of recurrent chromosomal gains and losses in primary nasopharyngeal carcinoma by comparative genomic hybridisation. *Int J Cancer* 82(4):498–503.
9. Alexandrov LB, et al.; Australian Pancreatic Cancer Genome Initiative; ICGC Breast Cancer Consortium; ICGC MMML-Seq Consortium; ICGC PedBrain (2013) Signatures of mutational processes in human cancer. *Nature* 500(7463):415–421.
10. Roberts SA, et al. (2013) An APOBEC cytidine deaminase mutagenesis pattern is widespread in human cancers. *Nat Genet* 45(9):970–976.
11. Swanton C, McGranahan N, Starrett GJ, Harris RS (2015) APOBEC enzymes: Mutagenic fuel for cancer evolution and heterogeneity. *Cancer Discov* 5(7):704–712.
12. Sasaki MM, et al. (2015) Integrated genomic analysis suggests MLL3 is a novel candidate susceptibility gene for familial nasopharyngeal carcinoma. *Cancer Epidemiol Biomarkers Prev* 24(8):1222–1228.
13. Sun SC (2010) CYLD: A tumor suppressor deubiquitinase regulating NF-kappaB activation and diverse biological processes. *Cell Death Differ* 17(1):25–34.
14. Massoumi R (2011) CYLD: A deubiquitination enzyme with multiple roles in cancer. *Future Oncol* 7(2):285–297.
15. Anonymous; Cancer Genome Atlas Network (2015) Comprehensive genomic characterization of head and neck squamous cell carcinomas. *Nature* 517(7536):576–582.
16. Hymowitz SG, Wertz IE (2010) A20: From ubiquitin editing to tumour suppression. *Nat Rev Cancer* 10(5):332–341.
17. Napetschnig J, Wu H (2013) Molecular basis of NF-κB signaling. *Annu Rev Biophys* 42:443–468.
18. Kan R, et al. (2015) NF-κB p65 subunit is modulated by latent transforming growth factor-β binding protein 2 (LTBP2) in nasopharyngeal carcinoma HONE1 and HK1 cells. *PLoS One* 10(5):e0127239.
19. Jacobs MD, Harrison SC (1998) Structure of an IkappaBalpha/NF-kappaB complex. *Cell* 95(6):749–758.
20. Spruck CH, 3rd, et al. (1992) Absence of p53 gene mutations in primary nasopharyngeal carcinomas. *Cancer Res* 52(17):4787–4790.
21. Cooper NR, Bradt BM, Rhim JS, Nemerow GR (1990) CR2 complement receptor. *J Invest Dermatol* 94(6 Suppl):112S–117S.
22. Dodd LE, et al. (2006) Genes involved in DNA repair and nitrosamine metabolism and those located on chromosome 14q32 are dysregulated in nasopharyngeal carcinoma. *Cancer Epidemiol Biomarkers Prev* 15(11):2216–2225.
23. McGranahan N, et al. (2015) Clonal status of actionable driver events and the timing of mutational processes in cancer evolution. *Sci Transl Med* 7(283):283ra54.
24. Harki DA, et al. (2015) Small molecule inhibitors of apobec3g and apobec3b. Patent Cooperation Treaty Appl WO 2015106272 A1 (July 16, 2015).
25. Petitjean A, et al. (2007) Impact of mutant p53 functional properties on TP53 mutation patterns and tumor phenotype: Lessons from recent developments in the IARC TP53 database. *Hum Mutat* 28(6):622–629.
26. Chung GT, et al. (2013) Constitutive activation of distinct NF-κB signals in EBV-associated nasopharyngeal carcinoma. *J Pathol* 231(3):311–322.
27. Dawson CW, Port RJ, Young LS (2012) The role of the EBV-encoded latent membrane proteins LMP1 and LMP2 in the pathogenesis of nasopharyngeal carcinoma (NPC). *Semin Cancer Biol* 22(2):144–153.
28. Cerami E, et al. (2012) The cBio cancer genomics portal: An open platform for exploring multidimensional cancer genomics data. *Cancer Discov* 2(5):401–404.
29. Hsu JL, Glaser SL (2000) Epstein-barr virus-associated malignancies: Epidemiologic patterns and etiologic implications. *Crit Rev Oncol Hematol* 34(1):27–53.
30. Park S, et al. (2007) The impact of Epstein-Barr virus status on clinical outcome in diffuse large B-cell lymphoma. *Blood* 110(3):972–978.
31. Sasaki N, et al. (2001) Nuclear factor-kappaB p65 (RelA) transcription factor is constitutively activated in human gastric carcinoma tissue. *Clin Cancer Res* 7(12):4136–4142.
32. Jost PJ, Ruland J (2007) Aberrant NF-kappaB signaling in lymphoma: Mechanisms, consequences, and therapeutic implications. *Blood* 109(7):2700–2707.
33. Liu X, et al. (2010) Mutations of NFKBIA in biopsy specimens from Hodgkin lymphoma. *Cancer Genet Cytogenet* 197(2):152–157.
34. Anonymous; Cancer Genome Atlas Research Network (2014) Comprehensive molecular characterization of gastric adenocarcinoma. *Nature* 513(7517):202–209.
35. Baud V, Karin M (2009) Is NF-kappaB a good target for cancer therapy? Hopes and pitfalls. *Nat Rev Drug Discov* 8(1):33–40.
36. Le Gallo M, et al.; NIH Intramural Sequencing Center (NISC) Comparative Sequencing Program (2012) Exome sequencing of serous endometrial tumors identifies recurrent somatic mutations in chromatin-remodeling and ubiquitin ligase complex genes. *Nat Genet* 44(12):1310–1315.
37. Li H, Durbin R (2009) Fast and accurate short read alignment with Burrows-Wheeler transform. *Bioinformatics* 25(14):1754–1760.
38. McKenna A, et al. (2010) The Genome Analysis Toolkit: A MapReduce framework for analyzing next-generation DNA sequencing data. *Genome Res* 20(9):1297–1303.
39. DePristo MA, et al. (2011) A framework for variation discovery and genotyping using next-generation DNA sequencing data. *Nat Genet* 43(5):491–498.
40. Van der Auwera GA, et al. (2013) From FastQ data to high confidence variant calls: The Genome Analysis Toolkit best practices pipeline. *Curr Protoc Bioinformatics* 43:11.10.1–11.10.33.
41. Purcell S, et al. (2007) PLINK: A tool set for whole-genome association and population-based linkage analyses. *Am J Hum Genet* 81(3):559–575.
42. Chang CC, et al. (2015) Second-generation PLINK: Rising to the challenge of larger and richer datasets. *Gigascience* 4:7.
43. Cibulskis K, et al. (2013) Sensitive detection of somatic point mutations in impure and heterogeneous cancer samples. *Nat Biotechnol* 31(3):213–219.
44. Koboldt DC, et al. (2012) VarScan 2: Somatic mutation and copy number alteration discovery in cancer by exome sequencing. *Genome Res* 22(3):568–576.
45. Fuentes Fajardo KV, et al.; NISC Comparative Sequencing Program (2012) Detecting false-positive signals in exome sequencing. *Hum Mutat* 33(4):609–613.
46. Dai W, et al. (2016) Whole-exome sequencing identifies MST1R as a genetic susceptibility gene in nasopharyngeal carcinoma. *Proc Natl Acad Sci USA* 113(12):3317–3322.
47. Moffat J, et al. (2006) A lentiviral RNAi library for human and mouse genes applied to an arrayed viral high-content screen. *Cell* 124(6):1283–1298.
48. Cheung AK, et al. (2013) Polo-like kinase inhibitor Ro5203280 has potent antitumor activity in nasopharyngeal carcinoma. *Mol Cancer Ther* 12(8):1393–1401.
49. Shuen WH, Kan R, Yu Z, Lung HL, Lung ML (2015) Novel lentiviral-inducible transgene expression systems and versatile single-plasmid reporters for in vitro and in vivo cancer biology studies. *Cancer Gene Ther* 22(4):207–214.